STEM CELLS AND DEVELOPMENT
Volume 23, Number 2, 2014

DOI: 10.1089/scd.2013.0097

Spheroid Culture for Enhanced Differentiation of Human Embryonic Stem Cells to Hepatocyte-Like Cells

Kartik Subramanian,[1,*] Derek Jason Owens,[1,*] Ravali Raju,[1,*] Meri Firpo,[2] Timothy D. O'Brien,[2] Catherine M. Verfaillie,[3] and Wei-Shou Hu[1]

Stem cell-derived hepatocyte-like cells hold great potential for the treatment of liver disease and for drug toxicity screening. The success of these applications hinges on the generation of differentiated cells with high liver specific activities. Many protocols have been developed to guide human embryonic stem cells (hESCs) to differentiate to the hepatic lineage. Here we report cultivation of hESCs as three-dimensional aggregates that enhances their differentiation to hepatocyte-like cells. Differentiation was first carried out in monolayer culture for 20 days. Subsequently cells were allowed to self-aggregate into spheroids. Significantly higher expression of liver-specific transcripts and proteins, including Albumin, phosphoenolpyruvate carboxykinase, and asialoglycoprotein receptor 1 was observed. The differentiated phenotype was sustained for more than 2 weeks in the three-dimensional spheroid culture system, significantly longer than in monolayer culture. Cells in spheroids exhibit morphological and ultrastructural characteristics of primary hepatocytes by scanning and transmission electron microscopy in addition to mature functions, such as biliary excretion of metabolic products and cytochrome P450 activities. This three-dimensional spheroid culture system may be appropriate for generating high quality, functional hepatocyte-like cells from ESCs.

Introduction

Treatments for end stage liver failure are largely dependent on liver organ or hepatocyte cell transplantation, which are limited by the availability of donor organs or cells [1–3]. Severe end-stage liver disease may benefit from an extracorporeal bioartificial liver (BAL) device as a bridge to liver transplantation or even regeneration [4,5]. However, such BAL devices for extracorporeal liver support have to resort to xenogeneic cell sources or tumorigenic cell lines because of the lack of human hepatocytes. A renewable cell source, especially stem cell-derived human hepatocytes, will greatly enhance the prospect of liver cell based therapy [6]. Stem cell-derived hepatocytes may also find applications in drug metabolism and toxicity studies [7–9]. Successful derivation of hepatocytes from pluripotent human stem cells will therefore, ensure virtually unlimited cell sources for discovery and clinical applications.

Human embryonic stem cells (hESCs) cultured under low adhesive conditions form aggregates called embryoid bodies (EBs). They have a propensity to spontaneously differentiate to multiple cell lineages, including the hepatic endoderm, but at a rather low efficiency [10]. In contrast directed and controlled differentiation to hepatic lineage has had more success in many laboratories [11–14]. These directed differentiation protocols entail plating of hESC on extracellular matrices and treatment with a series of cocktails of cytokines and growth factors to promote hepatic differentiation as evidenced by the presence of liver markers [15].

We recently described a 20-day, four stage protocol for differentiation of ES and induced pluripotent stem cells (iPS), from both human and mouse, to cells of hepatic lineage [11]. Cells grown to confluency on matrigel were guided toward definitive endoderm with Activin-A and Wnt3a, followed by specification to hepatic endoderm by treatment with bone morphogenetic protein (BMP)4 and basic fibroblast growth factor (bFGF), to bipotential hepatoblasts using aFGF, FGF4b, and FGF8, and finally toward a hepatocyte-like cell state by treatment with hepatocyte growth factor (HGF) and Follistatin. This stepwise treatment results in ~10%–20% of the cell population demonstrating a fetal hepatocyte-like with some characteristics of adult hepatocytes.

Others have used similar sets of growth factors invariably encompassing combinations of Activin A, Wnt3, bFGF, BMP-4, HGF, Oncostatin M, and/or Dexamethasone (Dex) [16,17]. The number of stages, in which different combinations of growth factors are used, differ somewhat, in various protocols, ranging from three to five.

Departments of [1]Chemical Engineering and Materials Science, [2]Stem Cell Institute, University of Minnesota, Minneapolis, Minnesota.
[3]Interdepartmental Stem Cell Institute, Catholic University Leuven, Leuven, Belgium.
*These authors contributed equally to this work.

The current directed differentiation protocols give rise to heterogeneous populations. The transcript levels of many key hepatic genes are still relatively low. The yields of hepatocyte-like cells, as well as their functional maturity, need to be further enhanced. Furthermore, the differentiated hepatic functions in those cells need to be sustained for a longer period for most applications.

Primary hepatocytes, when cultured on a surface with a decreased adhesiveness and at a subconfluent density, self-assemble into spheroids that exhibit enhanced levels of a variety of hepatic functions. They sustain hepatic functions over a longer period in culture than the monolayer culture [18,19].

We previously applied our differentiation protocol to direct the differentiation of rat multipotent adult progenitor cells cultivated as 3D aggregates to hepatic lineage. The resulting hepatocyte-like cells had higher liver specific functions, including albumin (*ALB*) and urea secretion and cytochrome P450 (*CYP450*) activity, than those obtained from monolayer culture [20]. Here we examined the effect of cultivation of hESCs in 3D spheroids on the maturation of the hepatocyte-like progeny. As hESCs differentiate spontaneously when cultivated as EBs, they were thus, first differentiated toward hepatic lineage in monolayer cultures for 20 days, and then formed spheroids. We report here the enhanced maturation and liver functions for hESC-derived hepatocyte like cells cultured as spheroids.

Materials and Methods

HESC culture

The hESC line HSF6 was cultured as previously described (1). Briefly, hESCs were maintained in Dulbecco's modified Eagle's medium (DMEM) (Gibco/BRL), 20% Knockout Serum Replacement (Gibco), 2 mM glutamine, 0.1 mM nonessential amino acids, 0.1 mM β-mercaptoethanol, and bFGF (R&D) (4 ng/mL) on mouse embryonic fibroblasts (MEFs). MEFs were derived from E13–E14 CF-1 mice (Charles River Laboratories) and mitotically inactivated using gamma radiation (3,000 rads). hESCs were plated on the MEFs and cultured in hESC medium at 37°C in 10% CO_2. The cells were routinely passaged using 0.1% (w/v) Collagenase Type IV (Gibco) in ES basal media every 3–5 days.

Hepatocyte differentiation

HSF6 cells were plated in 12 well plates, precoated with 2% matrigel (BD Biosciences) in MEF-conditioned media (CM) until 50% confluency was reached. To initiate differentiation, the CM was aspirated, the cells were washed once with PBS, and differentiation medium was added. The differentiation basal medium consisted of a 60/40 (v/v) mixture of low glucose DMEM (Gibco) and MCDB-201 (Sigma), and supplemented with 0.026 μg/mL ascorbic acid 3-phosphate (Sigma), linoleic acid bovine serum albumin (LA-BSA; Sigma) (1 mg/mL BSA and 8.13 μg/mL LA), insulin-transferrin-selenium (Sigma) (2.5 μg/mL insulin, 1.38 μg/mL transferrin, 1.25 ng/mL sodium selenite), 0.4 μg/mL Dex (Sigma), 4.3 μg/mL β-mercaptoethanol (Hyclone), 100 IU/mL penicillin and 100 μg/mL streptomycin (Gibco) and qualified fetal bovine serum [2% (v/v) for the first 6 days and 0.5% (v/v) for the subsequent time period).

Cytokines and growth factor were supplemented as follows: (1) D0: Activin A (100 ng/mL) and Wnt3a (50 ng/mL) (2) D6: bFGF (10 ng/mL) and BMP4 (50 ng/mL) (3) D10: FGF8b (25 ng/mL), aFGF (50 ng/mL) and FGF4 (10 ng/mL) (4) D14: HGF (20 ng/mL) and Follistatin (100 ng/mL). 50% media change was performed every 2 days using medium of the corresponding differentiation stage. On D0, D6, D10, and D14, medium was completely replaced with fresh medium of the ensuing differentiation stage after a brief rinse with PBS.

Formation of hepatic spheroids

Cells were detached after treatment with 0.1% (w/v) collagenase (type IV) (Invitrogen) for 15–20 min at 37°C. After centrifugation (1,000 rpm 5 min) the cell pellet was treated with 0.05% (w/v) trypsin with 2% (v/v) chicken serum (37°C, 10 min). The cell suspension was then passed through a 100 μm nylon mesh to obtain a single cell suspension.

Approximately 8,000 cells in 100 μL of stage IV differentiation medium was added to each well of an ultra-low attachment (ULA) round bottomed 96 well plate (Corning). After centrifugation for 4 min at 1,500 rpm (400*g*), cells settled to the bottom of the well to form spheroids in the following 2 to 3 days.

Characterization of spheroids

Quantitative real time PCR was used to measure the transcript levels of hepatic genes. Flow cytometry was used to quantify the cell fraction exhibiting mature hepatic markers using antibodies for asialoglycoprotein receptor (*ASGPR*; Thermoscientific, 1:10 dilution) and phosphoenolpyruvate carboxykinase (*PEPCK*; Santa-Cruz, H-300, 1:2,000 dilution). The secondary antibodies used were anti-mouse IgG1 A488 labeled (Molecular Probes, 1:500 dilution) and anti-rabbit IgG A488 (Molecular Probes, 1:500 dilution). The secretion of *ALB* was measured by Enzyme-linked immunosorbent assay and CYP450 activities were imaged and quantified by biotransformation of fluorogenic substrate [21]. Biliary secretion was monitored through fluorescein activity. Ultrastructural features were assessed using scanning and transmission electron microscopy (TEM). Details of these assays can be found in Supplementary Material and Methods section; Supplementary Data are available online at www.liebertpub.com/scd

Results

Three-dimensional spheroid formation

The hESC line, HSF6, was differentiated towards the hepatic lineage as described [11]. On D20, cells were detached for formation of three-dimensional spheroids. Typically, we obtained 4×10^5 cells/cm^2 from the monolayer culture with high viability (>90%). Approximately 8,000 cells were added to each well of a U-bottom ULA culture plates. Over time ~40% of the cells in each well form multiple small clusters, which progressively agglomerate into larger clusters in 2 days. The viability immediately after seeding was very high (Fig. 1). At 24 h, cells within the clusters remained viable, while individual cells not in clusters were no longer viable. Subsequently cells in the cluster became more compact and the size of the aggregate decreases somewhat (Fig. 1a). Six days after the initiation of 3D formation (D26) the surface of

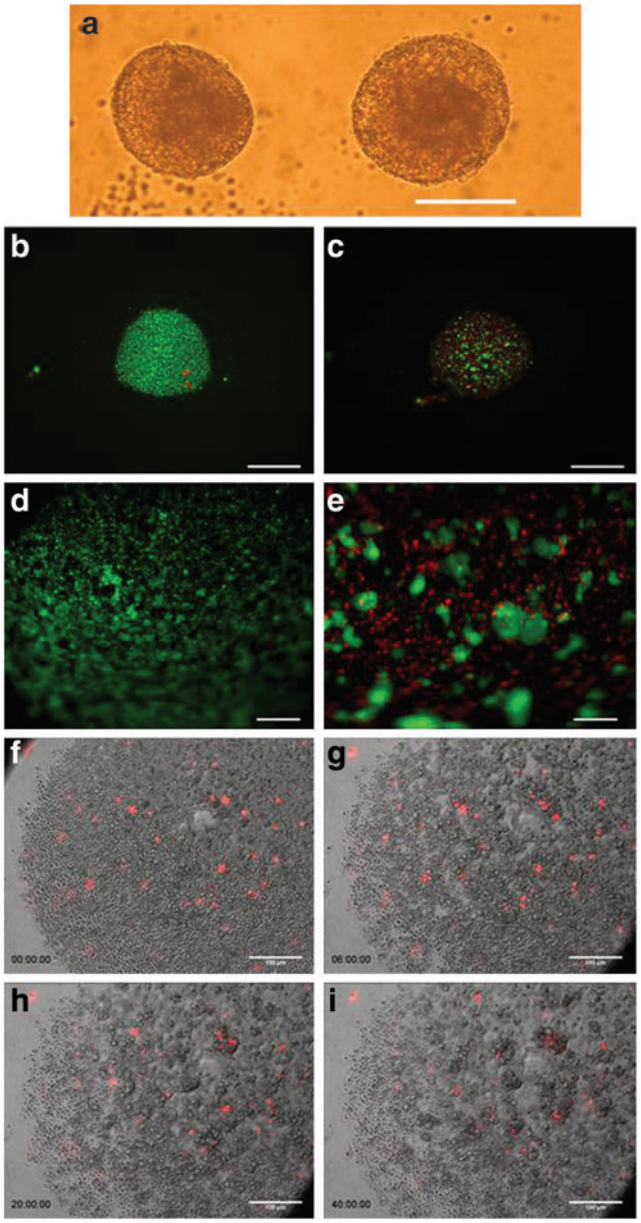

FIG. 1. Formation and characterization of 3D Spheroids **(a)** Morphology of human embryonic stem cell (hESC) derived 3D differentiated spheroids (Day 26), (scale bar 200 μm); **(b–e)** Live-dead viability staining during spheroid formation immediately after seeding on D20 (**b**, 2.5×; **d**, 10×) and 24 h after formation on D21 (**c**, 2.5×; **e**, 20×), live, viable cells labeled with green fluorescence, and nonviable cells labeled with red fluorescence (scale bars for **b** and **c** 400 μm, scale bars for **d** and **e** 100 μm); **(f–i)** Time-lapse images of spheroid formation with 1% of bulk population labeled with DiI membrane stain (scale bars 100 μm). Color images available online at www.liebertpub.com/scd

all the spheroids becomes relatively smooth. There is no evidence of cell proliferation. The diameter of the compacted spheroids ranges from 94 to 293 μm, with an average of about 150 μm (Supplementary Fig. S1). Additional images of spheroid formation on days D0 to D7 are shown in Supplementary Fig. S2.

Time-lapse microscopy was employed to directly observe the early stages of spheroid formation (Fig. 1f–i; Supplementary Video S1). A small fraction (1%) of the cells was labeled with Vybrant DiI membrane dye before they were placed into ULA well to facilitate the tracking of individual cells amongst the bulk population. Cells were seen to be incorporated into the aggregating cell clusters in proximity to their initial position. However, a small fraction of cells did move over distances, before being incorporated into an aggregate. These data suggest that cell incorporation into spheroids is not a random process, but selectively enriches viable cells.

Expression of hepatic genes in 3D spheroids

The expression of several hepatic-specific genes in spheroid culture was evaluated and compared to cells maintained in monolayer culture until D26. Results are presented as ratio of transcripts of D26 cells to D20 cells in monolayer culture (Fig. 2). The transcript levels for all liver specific genes tested increased in D26 spheroids from D20 and are higher compared to D26 monolayer cultures. Most notably the transcript level of UDP glucuronosyltransferase 1A1 (*UGT1A1*), a gene encoding an enzyme involved in bilirubin conjugation in the liver, increased about 60-fold in spheroids comparing to about 2-fold increase in monolayer culture. The level of *ALB* transcript increased by about 16-fold over the 6 days in spheroids, but remained relatively unchanged in monolayer culture. The level of increase was more moderate for other genes, including *arginase 1 (ARG1)*, an enzyme involved in the urea cycle, *hepatocyte nuclear factor 4a (HNF4a)*, a liver enriched transcription factor, *Factor VII (FVII)*, a member of coagulation factor family, and *connexin 32* (*CX32*), a gap junction protein. Nevertheless, the levels of transcripts of those genes were all higher than the levels in cells maintained in monolayer culture.

The expression level of most mature hepatic transcripts, including *ALB*, *ARG1*, *UGT1A1*, *HNF4a*, and *FVII* were maintained till D35 in the 3D spheroid culture (Fig. 3). In comparison, the expression levels of these genes in the monolayer culture either remained at a constant but lower level than the spheroid culture or decreased in the same period.

Expression of hepatic proteins in spheroids

The differentiation of ESCs to the hepatic lineage yields heterogeneous progeny containing cells with different degrees of hepatocyte maturation, as well as other less well-identified cells. We examined the expression of two mature liver specific proteins; *ASGPR-1* and *PEPCK* (Fig. 3g, h) in the spheroids by flow cytometry. *ASGPR-1* plays an important role in the uptake and degradation of glycoproteins with exposed terminal galactose or N-acetylgalatosamine, while *PEPCK* is a pivotal enzyme in gluconeogenesis in liver. On D20, ~16% of the hESC hepatic progeny were *ASGPR-1* positive. The fraction of *ASGPR-1* positive cells increased to 60% on D26, after spheroid formation. A similar increase with the fraction of cells staining positive for *PEPCK* was seen, from 17% on D20 to 70% on D26, and about 80% on D32. In both cases, the percentage of cells expressing the hepatic-specific proteins increased significantly in spheroid cultures. The presence of *PEPCK* protein was confirmed by immunostaining after cell permeabilization (Fig. 3i). Further immunohistochemistry on D32 spheroids for alpha-fetoprotein (*AFP*), *ALB, CK8,* and *CK18* is shown in Supplementary Fig. S3.

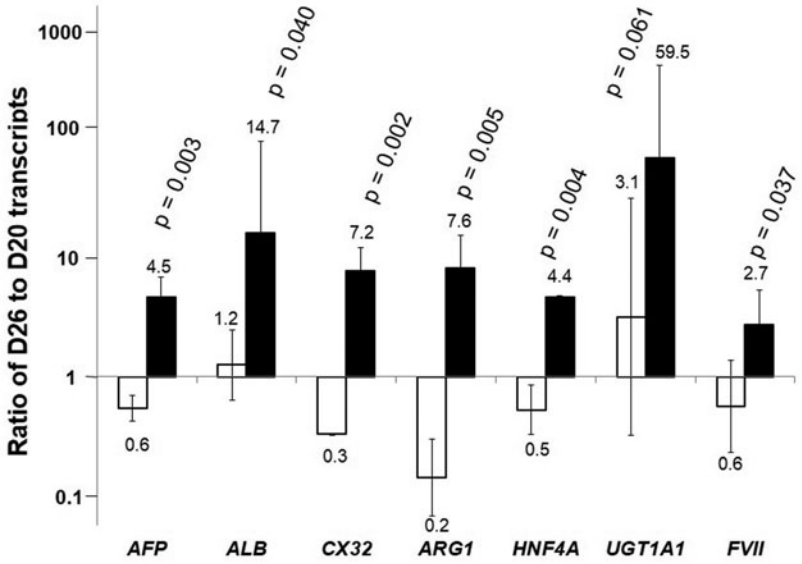

FIG. 2. Relative transcript levels in differentiated spheroids. Change in transcript level of liver specific genes on D26 relative to the starting cells at D20 for cells formed 3D spheroid (■) and maintained as monolayer (□) (average of $n=3$). The transcript levels were normalized to that of *GAPDH* of the same sample. The fold changes of gene expression in D26 cells relative to D20 cells are shown. The higher value thus, represents higher extent of increase in the transcript level.

Structural characteristics of spheroids

Under scanning electron microscopy (SEM), the spheroids appear densely packed; the boundaries of individual cells were nearly indistinguishable (Fig. 4a, b). A micrograph with a higher magnification is shown in Fig. 4b. Typical hepatocyte morphology can be seen on cell clusters on the exterior of the aggregate (Fig. 4c) with some polygonal cells exhibiting abundant microvilli on the cell surface (Fig. 4d).

TEM revealed that cells in the spheroids on D30 displayed the typical polygonal morphology with numerous microvilli

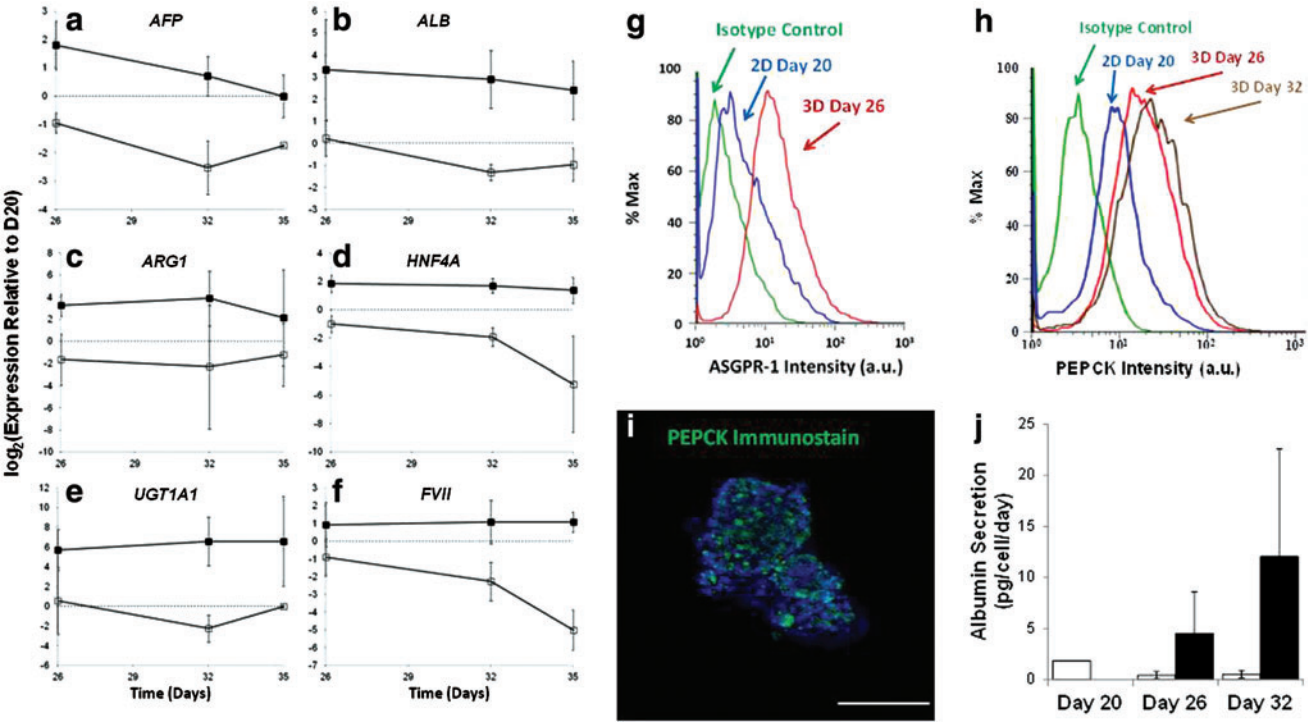

FIG. 3. Sustaining differentiated properties in spheroids. The level of transcript is expressed as a relative value to that at D20 in (■) spheroid culture; (□): monolayer culture (average of $n=3$) for **(a)** *AFP*; **(b)** *ALB*; **(c)** *ARG1*; **(d)** *HNF4A*; **(e)** *UGT1A1*; **(f)** *FVII*; (The expression level at D20 is marked with *dash line*)**; (g)** *ASGPR-1* expression by FACS analysis preceding spheroid formation at D20 (*blue*) and after at D26 (*red*) (isotype matched control in *green*); **(h)** Phosphoenolpyruvate carboxykinase (*PEPCK*) expression by FACS analysis at D20 (*blue*), D26 (*red*) and D32 (*brown*) (isotype matched control in *green*); **(i)** immunostaining (*green*) of *PEPCK* in spheroids with 4′,6-diamidino-2-phenylindole nuclear counter stain (*blue*) (scale bar, 50 μm); **(j)** Albumin secretion by enzyme-linked immunosorbent assay analysis in monolayer (□) and spheroid (■). Color images available online at www.liebertpub.com/scd

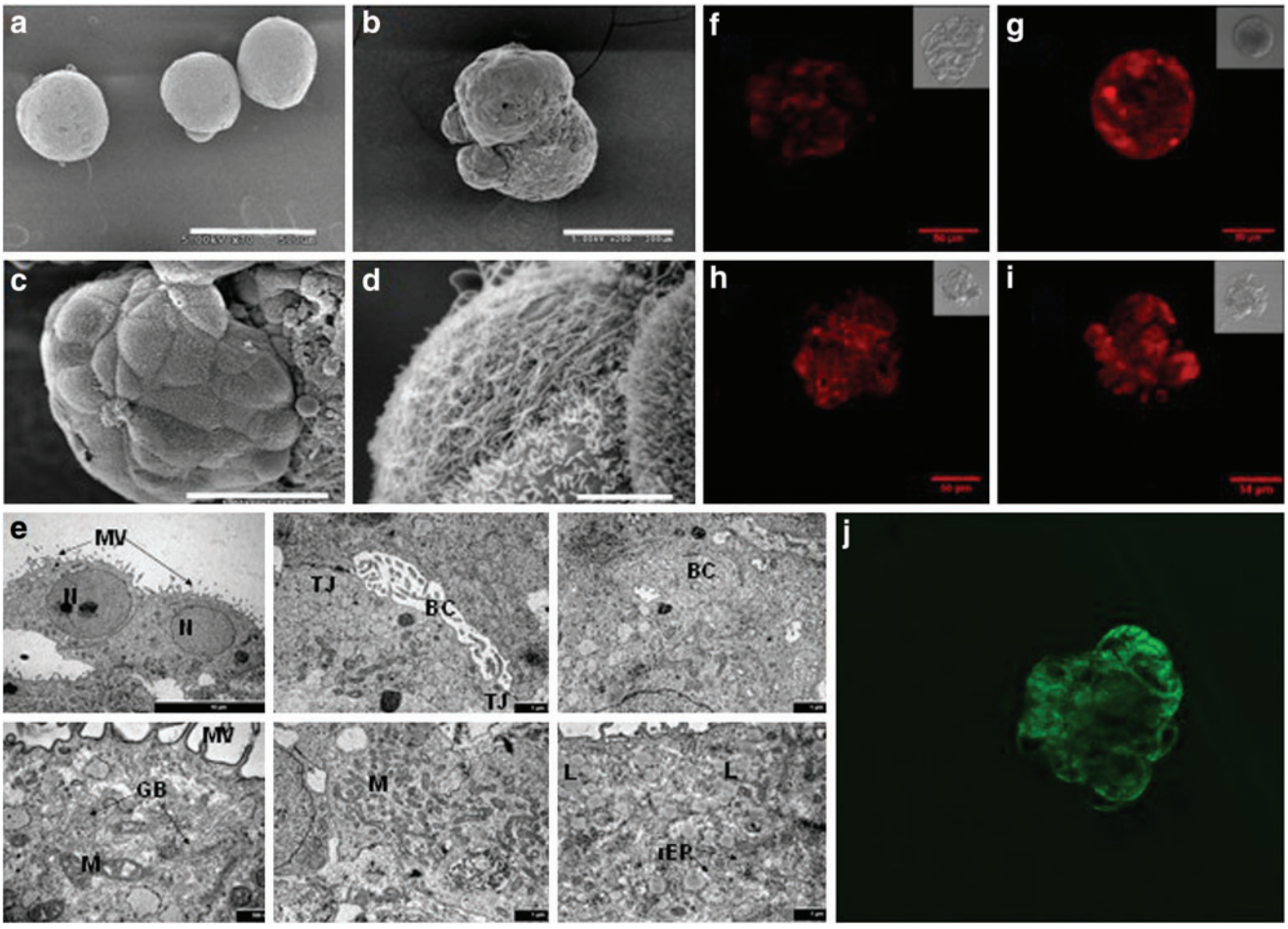

FIG. 4. Images of hESC derived hepatic-like cell spheroids. Scanning electron microscopy images of hESC derived spheroids on D30 at **(a)** 70× (scale bar, 500 μm), **(b)** 200× (scale bar, 200 μm), **(c)** 1,000× (scale bar, 50 μm), **(d)** 7,000× (scale bar, 5 μm). **(e)** Transmission electron microscopic micrographs of hESC-derived spheroids on D30. Labels: nucleus (N); microvilli (MV); bile-canaliculi (BC); tight junctions (TJ); golgi body (GB); mitochondria (M); lipid droplets (L); and rough endoplasmic reticulum (rER) (scale bars: *upper left panel*, 10 μm; *lower left panel*, 500 nm; all others 1 μm). **(f, g)** Accumulation of fluorescent resorufin from Ethoxyresorufin O-dealkylation reaction in D32 spheroids without **(f)** or with **(g)** 24 h of β-naphthoflavone treatment. **(h, i)** Accumulation of fluorescent resorufin from Pentoxyresorufin O-dealkylation reaction in D32 spheroids, without **(h)** or with **(i)** 24 h of phenobarbital treatment. *Insets* show transmitted light images of the spheroids (scale bars, 50 μm). **(j)** Polarized accumulation of fluorescein in hESC derived spheroids (scale bar, 50 μm). Color images available online at www.liebertpub.com/scd

(Fig. 4e). Intercellular bile-canaliculi delimited by tight junctions were also observed; Golgi apparatus, plentiful mitochondria, lipid droplets, and rough endoplasmic reticulum were all seen. Lysosomes and inter-cellular coated vesicles involved in degrading biological materials were also visible.

Hepatocytes exhibit polarized surface domains even in culture. In vivo they excrete bile acid into the bile canaliculi. In culture, they accumulate excreted chemical species in the space in between cells. Incubation with a dilute solution of fluorescein diacetate, which forms fluorescent fluorescein upon intracellular cleavage by esterase, results in an accumulation of excreted fluorescein in the intercellular space. This has been used as an indication of polarization of cellular surface domains [22,23]. Spheroids at D32 were incubated in 3 μg/mL of fluorescein diacetate, and the accumulation of fluorescein in the intercellular space was visible by confocal imaging (Fig. 4j), indicating cell polarization.

Functional activity of HESC derived spheroids

We next evaluated a number of hepatic activities in the hESC derived hepatocyte-like cells and compared the level in spheroids to that in cells maintained as monolayer. The cell numbers of spheroids in wells were enumerated and the average *ALB* secretion rate was estimated. *ALB* secretion rate, initially at 1.83 pg/cell/day on D20 before spheroid formation increased to 4.52 and 12.05 pg/cell/day on D26 and D32 respectively in spheroid culture, but subsided to 0.45 and 0.53 pg/cell/day in monolayer culture on D26 and D32 (Fig. 3j). Thus, spheroid formation resulted in a substantial increase in the ALB secretion rate, and the higher rate was sustained over the cultivation period.

We also assessed *Cyp1A1/2* and *Cyp2B6/7* activity by ethoxyresorufin-O-dealkylation (EROD) and pentoxyresorufin-O-dealkylation (PROD) reactions. The intracellular accumulation of the fluorescent resorufin after the cleavage of ethoxyresorufin or pentoxyresorufin, indicative of EROD

(Fig. 4g) and PROD (Fig. 4i) activities was seen in spheroids under confocal microscopy. The spheroids were then treated with β-napthoflavone and Phenobarbital, inducers of *Cyp1A1* and *Cyp2B6/7*, respectively. A modest increase in EROD activity after β-napthoflavone treatment (Fig. 4g) was observed, but little change was observed in PROD activity after Phenobarbital treatment (Fig. 4i).

EROD and PROD activities were also quantified by measuring the rate of resorufin product release into the media (Supplementary Fig. S4a, b). Resorufin release increased nearly five-fold after β-napthoflavone induction but not after Rifampicin treatment (EROD assay). Likewise, resorufin release increased marginally after treatment with Phenobarbital but not Rifampicin (PROD assay).

To further interrogate the phenomenon of specific *CYP450* activity, the expression of the relevant CYP450 gene products were evaluated by quantitative PCR with or without drug treatment (Supplementary Fig. S4c, d). *Cyp1a1* transcript expression increased 24-fold after 24 h of β-napthoflavone induction, while Rifampicin treatment resulted in minimal change in *Cyp1a1* expression. Thus, consistent results were seen for intracellular accumulation and excretion of resorufin and transcript levels for the specific Cyp450: induction of *Cyp1A1/2* expression and function by β-napthoflavone, but no increase in expression and function of *Cyp2B6/7* by Phenobarbital.

Discussion

In this study, we extended our monolayer hESC differentiation into three-dimensional spheroid culture. After a 20-day differentiation that directed cells to the hepatic lineage, cultivation of the cells as spheroids resulted in enhanced expression of many hepatic lineage markers. This was illustrated by the increased gene expression at the transcript level for a number of liver specific genes, including *UGT1A1* and *ARG1* (Fig. 2) and protein levels for the intracellular enzyme *PEPCK* and cell surface protein *ASGPR1*, and secreted *ALB* (Fig. 3).

The 3D spheroid culture system also allowed maintenance of the differentiation markers for an extended period. During extended culture for 15 days in the spheroid system, expression levels of hepatic-specific transcripts were maintained at the level achieved after 6 days of spheroid culture (Fig. 3). In contrast, the expression levels of hepatic transcripts in cells that were maintained in monolayer culture significantly decreased between D26 and D35. The results suggest that the observed enhanced differentiation was not merely an outcome of the extended culture period. It is more probable that the process of self-assembly and the tissue-like 3D structure in the spheroid has a positive effect in the hepatic differentiation.

After nearly 2 weeks in spheroid culture, hepatocyte-like cells derived from hESCs still exhibited biological activity of *Cyp1A1/2* and *Cyp2B6/7* enzymes as shown by EROD and PROD reactions (Fig. 4). Cyp450 activities, responsible for the biotransformation of many xenobiotics and the metabolism of drugs, are vital functions in liver. Many of those enzyme activities are induced by chemical inducers both in vivo and in vitro in cultured hepatocytes. We demonstrated that *Cyp1A1/2* gene expression and enzyme function in the spheroid cultures responded to the induction by β-Napthoflavone. The increased activity was seen in the accumulation of resorufin product within the spheroids (Fig. 4), in the release of resorufin into the media (Supplementary Fig. 4a, b), and expression of the gene transcripts (Supplementary Fig. 4c, d). However, the *Cyp2B6/7* activity as measured by the PROD reaction did not respond to treatment with the specific inducer Phenobarbital. The results are similar to what others have observed in hepatocyte-like cells derived from different stem cell systems, showing the inducibility of *Cyp1A2* level [16,17,24] but the lack of inducibility in *Cyp2B6* level [16,24].

Some hepatocyte-like cells exhibit morphology markedly similar to mature hepatocyte in SEM (Fig. 4b, c), although heterogeneity in morphology is also visible. Ultrastructurally, the cells in the spheroids also exhibit features expected in mature liver cells, especially microvilli aligning the canaliculi like openings. The extensive cell-cell interactions are visible in TEM micrographs (Fig. 4e). The spatial polarization is observed by secretion of fluorescein (Fig. 4j). The ultrastructure did not reveal any necrosis despite the 100–150 μm size range. In previous studies with primary hepatocytes (19) and rat adult bone marrow derived stem cells (21), high viability was seen in spheroids with a similar size range. How the viability or ultrastructure is affected by different seeding cell densities is yet to be explored. The structural characteristics of these spheroids show some resemblance to hepatocytes, which is consistent with the enhanced hepatocyte properties at transcript, protein and functional levels.

Three-dimensional culture systems have been shown to promote enhanced cellular structure and function in many cell and tissue types, including mammary epithelial cells [25], mesenchymal stem cells [26], neural cells [27], and hepatic cells [19,28–34]. In those studies employing mouse, rat or pig primary hepatocytes, cells were allowed to adhere to moderate to low attachment surface to enhance spheroid formation [33,35]. In other studies, primary hepatocytes were cultivated in suspension with a stirred bioreactor to form spheroids [36,37]. We recently reported three-dimensional aggregate differentiation of rat multipotent adult progenitor cells by allowing them to agglomerate in low attachment plates. Increased transcript expression of liver specific genes, ALB secretion, and enhanced activities of some CYP450 and more profound ultrastructural characteristics of liver tissue were observed as compared to the differentiation carried out in monolayer culture [20].

In our differentiations, D20 cells mostly consist of a mixture of fetal and adult hepatocyte like cells [11]. There are likely other cell types present in the differentiated culture, as suggested by the presence of *AFP*, *PEPCK* and *ASGPR-1* negative cells in the population by flow cytometric assays (Fig. 3). Transcript expression suggests presence of some endothelial cells (*VE-cadherin*) although other lineage markers, such as *SM22* (smooth muscle) and *Nkx2.5* (pancreas) remain relatively unchanged from D0 (Supplementary Fig. S5).

Similar multistage differentiations from hESC and human iPS cells toward hepatic lineages all yield cells expressing apparently similar transient levels of *AFP* and *ALB*, with levels of *ALB* expression similar to or exceeding expression in primary hepatocytes [16,17,38]. *AFP* is expressed in fetal liver cells but not in adult hepatocytes. In our case, the persistent

expression of *AFP*, thus, suggests the presence of immature fetal hepatocyte-like cells in the spheroids. Furthermore, some nonhepatic cells are likely still present within the spheroids and contribute to the heterogeneity of the cell population as seen in flow cytometric assays.

Flow cytometry for *ASGPR-1* clearly demonstrated a definite enrichment of *ASGPR-1* expressing cells on Day 26 of the 3D spheroid culture as compared to the Day 20 2D culture. Likewise, the enrichment in the fraction of *PEPCK* expressing cells from ~17% in the Day 20 samples to about 70% in Day 32 samples was also observed. Such increase in the fraction of more mature hepatocyte-like cells could be the results of spheroid formation. Another possibility of the enrichment of more mature cells in the initial phase of cell agglomeration is through specific cell-cell interactions.

The enhancement of both the fraction of differentiated cells and the liver specific gene expression through spheroid formation, although significant, still falls short of reaching the state of mature hepatocytes. This has been seen in all reports of hepatic lineage differentiation from embryonic and other stem cells. Recently, it was shown that overexpression of exogenous *FOXA2* and *HNF1a* via adenoviral vectors in differentiating hESC or hiPSC increases the percentage of cells reaching a more mature liver phenotype [24]. *ALB* expression in the differentiated progeny suggested that a very high percentage of cells exhibit hepatocyte characteristics with slight enhancement of CYP450 activities. Thus, enhancing functional maturity through overexpression of hepatic transcription factors or genes may be worth exploring

In summary, we have developed a simple and reproducible differentiation method consisting of step-wise monolayer based directed differentiation to the hepatic endoderm for 20 days, followed by a process of spontaneous self-assembly of cells into three-dimensional spheroids that can be maintained for at least an additional 15 days. This culture system not only improves the phenotypic and functional maturity of the differentiated cell population, but also allows for a more efficient maintenance of the cells for an extended culture time. This approach may thus, find application in high-throughput drug screening, in BAL support devices, as well as in hepatocyte transplantation.

Acknowledgments

K.S. was supported by a Graduate School fellowship from University of Minnesota. D.J.O. was supported by an NSF fellowship, Graduate School fellowship from University of Minnesota and a NIH Biotechnology Training Grant (GM08347). The support [EC-FP7-HeMiBio, FWO-c2685-g.0975.11] to C.M.V. is also acknowledged.

Author Disclosure Statement

No competing financial interests exist.

References

1. Jeon H and SG Lee. (2010). Living donor liver transplantation. Curr Opin Organ Transplant 15:283–287.
2. Hughes RD, RR Mitry and A Dhawan. (2012). Current status of hepatocyte transplantation. Transplantation 93:342–347.
3. Soltys KA, A Soto-Gutierrez, M Nagaya, KM Baskin, M Deutsch, R Ito, BL Shneider, R Squires, J Vockley, et al. (2010). Barriers to the successful treatment of liver disease by hepatocyte transplantation. J Hepatol 53:769–774.
4. Carpentier B, A Gautier and C Legallais. (2009). Artificial and bioartificial liver devices: present and future. Gut 58:1690–1702.
5. Nyberg SL. (2012). Bridging the gap: advances in artificial liver support. Liver Transpl 18 Suppl 2:S10–S14.
6. Haridass D, N Narain and M Ott. (2008). Hepatocyte transplantation: waiting for stem cells. Curr Opin Organ Transplant 13:627–632.
7. Sartipy P, P Bjorquist, R Strehl and J Hyllner. (2007). The application of human embryonic stem cell technologies to drug discovery. Drug Discov Today 12:688–699.
8. Dalgetty DM, CN Medine, JP Iredale and DC Hay. (2009). Progress and future challenges in stem cell-derived liver technologies. Am J Physiol Gastrointest Liver Physiol 297:G241–G248.
9. Jensen J, J Hyllner and P Bjorquist. (2009). Human embryonic stem cell technologies and drug discovery. J Cell Physiol 219:513–519.
10. Imamura T, L Cui, R Teng, K Johkura, Y Okouchi, K Asanuma, N Ogiwara and K Sasaki. (2004). Embryonic stem cell-derived embryoid bodies in three-dimensional culture system form hepatocyte-like cells *in vitro* and *in vivo*. Tissue Eng 10:1716–1724.
11. Roelandt P, KA Pauwelyn, P Sancho-Bru, K Subramanian, B Bose, L Ordovas, K Vanuytsel, M Geraerts, M Firpo, et al. (2010). Human embryonic and rat adult stem cells with primitive endoderm-like phenotype can be fated to definitive endoderm, and finally hepatocyte-like cells. PLoS One 5:e12101.
12. Agarwal S, KL Holton and R Lanza. (2008). Efficient differentiation of functional hepatocytes from human embryonic stem cells. Stem Cells 26:1117–1127.
13. Si-Tayeb K, FK Noto, M Nagaoka, J Li, MA Battle, C Duris, PE North, S Dalton and SA Duncan. (2009). Highly efficient generation of human hepatocyte-like cells from induced pluripotent stem cells. Hepatology 51:297–305.
14. Touboul T, NR Hannan, S Corbineau, A Martinez, C Martinet, S Branchereau, S Mainot, H Strick-Marchand, R Pedersen, et al. (2010). Generation of functional hepatocytes from human embryonic stem cells under chemically defined conditions that recapitulate liver development. Hepatology 51:1754–1765.
15. Snykers S, J De Kock, V Rogiers and T Vanhaecke. (2009). *In vitro* differentiation of embryonic and adult stem cells into hepatocytes: state of the art. Stem Cells 27:577–605.
16. Asgari S, M Moslem, K Bagheri-Lankarani, B Pournasr, M Miryounesi and H Baharvand. (2011). Differentiation and transplantation of human induced pluripotent stem cell-derived hepatocyte-like cells. Stem Cell Rev 9:493–504.
17. Chen YF, CY Tseng, HW Wang, HC Kuo, VW Yang and OK Lee. (2012). Rapid generation of mature hepatocyte-like cells from human induced pluripotent stem cells by an efficient three-step protocol. Hepatology 55:1193–1203.
18. Peshwa MV, FJ Wu, HL Sharp, FB Cerra and WS Hu. (1996). Mechanistics of formation and ultrastructural evaluation of hepatocyte spheroids. In Vitro Cell Dev Biol Anim 32:197–203.
19. Tostoes RM, SB Leite, M Serra, J Jensen, P Bjorquist, MJ Carrondo, C Brito and PM Alves. (2012). Human liver cell spheroids in extended perfusion bioreactor culture for repeated-dose drug testing. Hepatology 55:1227–1236.
20. Subramanian K, DJ Owens, TD O'Brien, CM Verfaillie and WS Hu. (2011). Enhanced differentiation of adult bone

marrow-derived stem cells to liver lineage in aggregate culture. Tissue Eng Part A 17:2331–2341.
21. Tzanakakis ES, CC Hsiao, T Matsushita, RP Remmel and WS Hu. (2001). Probing enhanced cytochrome P450 2B1/2 activity in rat hepatocyte spheroids through confocal laser scanning microscopy. Cell Transplant 10:329–342.
22. Bravo P, V Bender and D Cassio. (1998). Efficient *in vitro* vectorial transport of a fluorescent conjugated bile acid analogue by polarized hepatic hybrid WIF-B and WIF-B9 cells. Hepatology 27:576–583.
23. Oude Elferink RP, DK Meijer, F Kuipers, PL Jansen, AK Groen and GM Groothuis. (1995). Hepatobiliary secretion of organic compounds; molecular mechanisms of membrane transport. Biochim Biophys Acta 1241:215–268.
24. Takayama K, M Inamura, K Kawabata, M Sugawara, K Kikuchi, M Higuchi, Y Nagamoto, H Watanabe, K Tashiro, et al. (2012). Generation of metabolically functioning hepatocytes from human pluripotent stem cells by FOXA2 and HNF1alpha transduction. J Hepatol 57:628–636.
25. Weaver VM, S Lelievre, JN Lakins, MA Chrenek, JC Jones, F Giancotti, Z Werb and MJ Bissell. (2002). beta4 integrin-dependent formation of polarized three-dimensional architecture confers resistance to apoptosis in normal and malignant mammary epithelium. Cancer Cell 2:205–216.
26. Frith JE, B Thomson and PG Genever. (2010). Dynamic three-dimensional culture methods enhance mesenchymal stem cell properties and increase therapeutic potential. Tissue Eng Part C Methods 16:735–749.
27. Simao D, I Costa, M Serra, J Schwarz, C Brito and PM Alves. (2011). Towards human central nervous system *in vitro* models for preclinical research: strategies for 3D neural cell culture. BMC Proc 5 Suppl 8:P53.
28. Landry J, D Bernier, C Ouellet, R Goyette and N Marceau. (1985). Spheroidal aggregate culture of rat liver cells: histotypic reorganization, biomatrix deposition, and maintenance of functional activities. J Cell Biol 101:914–923.
29. Kelm JM, NE Timmins, CJ Brown, M Fussenegger and LK Nielsen. (2003). Method for generation of homogeneous multicellular tumor spheroids applicable to a wide variety of cell types. Biotechnol Bioeng 83:173–180.
30. Keller PJ, F Pampaloni and EH Stelzer. (2006). Life sciences require the third dimension. Curr Opin Cell Biol 18:117–124.
31. Griffith LG and MA Swartz. (2006). Capturing complex 3D tissue physiology *in vitro*. Nat Rev Mol Cell Biol 7:211–224.
32. Cukierman E, R Pankov, DR Stevens and KM Yamada. (2001). Taking cell-matrix adhesions to the third dimension. Science 294:1708–1712.
33. Abu-Absi SF, JR Friend, LK Hansen and WS Hu. (2002). Structural polarity and functional bile canaliculi in rat hepatocyte spheroids. Exp Cell Res 274:56–67.
34. Leite SB, I Wilk-Zasadna, JM Zaldivar, E Airola, MA Reis-Fernandes, M Mennecozzi, C Guguen-Guillouzo, C Chesne, C Guillou, PM Alves and S Coecke. (2012). Three-dimensional HepaRG model as an attractive tool for toxicity testing. Toxicol Sci 130:106–116.
35. Tsuchiya A, T Heike, H Fujino, M Shiota, K Umeda, M Yoshimoto, Y Matsuda, T Ichida, Y Aoyagi and T Nakahata. (2005). Long-term extensive expansion of mouse hepatic stem/progenitor cells in a novel serum-free culture system. Gastroenterology 128:2089–2104.
36. Lazar A, HJ Mann, RP Remmel, RA Shatford, FB Cerra and WS Hu. (1995). Extended liver-specific functions of porcine hepatocyte spheroids entrapped in collagen gel. In Vitro Cell Dev Biol Anim 31:340–346.
37. Wu FJ, JR Friend, CC Hsiao, MJ Zilliox, WJ Ko, FB Cerra and WS Hu. (1996). Efficient assembly of rat hepatocyte spheroids for tissue engineering applications. Biotechnol Bioeng 50:404–415.
38. Nakamura N, K Saeki, M Mitsumoto, S Matsuyama, M Nishio, M Hasegawa, Y Miyagawa, H Ohkita, N Kiyokawa, et al. (2012). Feeder-free and serum-free production of hepatocytes, cholangiocytes, and their proliferating progenitors from human pluripotent stem cells: application to liver-specific functional and cytotoxic assays. Cell Reprogram 14:171–185.

Address correspondence to:
Dr. Wei-Shou Hu
Department of Chemical Engineering and Materials Science
University of Minnesota
421 Washington Avenue SE
Minneapolis, MN 55455-0132

E-mail: acre@cems.umn.edu

Received for publication February 14, 2013
Accepted after revision September 8, 2013
Prepublished on Liebert Instant Online September 11, 2013